THE JOURNAL OF BIOLOGICAL CHEMISTRY VOL. 287, NO. 8, pp. 5211–5224, February 17, 2012

Dentin Phosphoprotein (DPP) Activates Integrin-mediated Anchorage-dependent Signals in Undifferentiated Mesenchymal Cells*[S]

Received for publication, August 8, 2011, and in revised form, November 21, 2011 Published, JBC Papers in Press, December 1, 2011, DOI 10.1074/jbc.M111.290080

Asha Eapen, Amsaveni Ramachandran, and Anne George[1]

From the Brodie Tooth Development Genetics and Regenerative Medicine Research Laboratory, Department of Oral Biology, University of Illinois, Chicago, Illinois 60612

Background: DPP mediates activation of anchorage-dependent signals.
Results: DPP activates focal adhesion complexes and MAPK signaling in undifferentiated mesenchymal cells and primary pulp cells, leading to their terminal differentiation into odontoblast-like cells.
Conclusion: DPP on the substrate provides a tight association between the structural and signaling elements in undifferentiated mesenchymal cells.
Significance: DPP promotes adhesion-based odontogenic cell differentiation.

Dentin phosphoprotein (DPP), a major noncollagenous protein of the dentin matrix, is a highly acidic protein that binds Ca^{2+} avidly and is thus linked to matrix mineralization. Here, we demonstrate that the RGD domain in DPP can bind to integrins on the cell surface of undifferentiated mesenchymal stem cells and pulp cells. This coupling generates intracellular signals that are channeled along cytoskeletal filaments and activate the non-receptor tyrosine kinase focal adhesion kinase, which plays a key role in signaling at sites of cellular adhesion. The putative focal adhesion kinase autophosphorylation site Tyr^{397} is phosphorylated during focal adhesion assembly induced by DPP on the substrate. We further demonstrate that these intracellular signals propagate through the cytoplasm and activate anchorage-dependent ERK signaling. Activated ERK translocates to the nucleus and phosphorylates the transcription factor ELK-1, which in turn coordinates the expression of downstream target genes such as *DMP1* and dentin sialoprotein (*DSP*). These studies suggest a novel paradigm demonstrating that extracellular DPP can induce intracellular signaling that can be propagated to the nucleus and thus alter gene activities.

Dentin sialophosphoprotein (DSPP),[2] a member of the SIBLING family, is a noncollagenous protein synthesized by odontoblasts (1–3). Shortly after DSPP is synthesized, it is cleaved into three polypeptides, namely dentin sialoprotein (DSP) (2, 4), dentin glycoprotein (DGP), and dentin phosphoprotein (DPP) (1, 5). The mouse *DSPP* gene contains five exons and four introns with exons 1–4 and part of exon 5 encoding the DSP protein and the remainder of exon 5 encoding the DPP protein. Mutation in the *DSPP* gene has been identified to be associated with the genetic disease dentinogenesis imperfecta type II (6–9). *DSPP* knock-out mice displayed dentin defects with less mineralized dentin and wider unmineralized predentin (10). The intact DSPP protein has not yet been isolated from the dentin matrix. Published reports have shown the expression patterns of DSP and DPP as specific markers for terminally differentiated odontoblasts (11, 12).

DPP (also called "phosphophoryn") is a highly acidic protein and is the major noncollagenous matrix component of dentin (13–15). The molecule is so-called because it is considered to be a "phosphate carrier" (16). DPP is exceedingly rich in aspartic acid and serine residues $((DSS)_n)$, and about 90% of the serine residues are phosphorylated (17, 18). This enables DPP to have a strong affinity for calcium ion, and thus it significantly promotes the growth of hydroxyapatite crystals when bound to collagen fibrils *in vitro* (19–21). Published reports have implicated DPP as a signaling molecule like some members in the SIBLING family (22). Reports have shown that stimulation of MC3T3-E1 cells by DPP could drive cell differentiation into the osteoblast phenotype by activation of the MAPK pathway (23). The use of DPP conditional knock-out mice revealed the distinct roles of DSP and DPP in dentin mineralization (11).

DPP contains a conserved RGD domain at the N terminus, implicating a functional role in the initiation of integrin-mediated intracellular signaling pathways. The binding of ligands to integrin often triggers intracellular signals that are transmitted through the actin cytoskeleton by assembly of specialized structures called focal adhesions (24, 25). Focal adhesion kinase (FAK), a potential signaling molecule, associates with paxillin and can trigger a diverse downstream signaling cascade. Published reports have shown that the PI3K/Akt, c-Jun, and p53 pathways are some of the downstream signaling pathways that are activated (26, 27). Along with FAK, ELK-1, a member of the ETS domain transcription factor family, is thought to play a crucial role in the regulation of signaling cascades that ulti-

* This work was supported, in whole or in part, by National Institutes of Health Grant DE 19633. This work was also supported by the Brodie Endowment Fund.
[S] This article contains supplemental Figs. S1 and S2.
[1] To whom correspondence should be addressed. Tel.: 312-413-0738; Fax: 312-996-6044; E-mail: anneg@uic.edu.
[2] The abbreviations used are: DSPP, dentin sialophosphoprotein; FAK, focal adhesion kinase; DPP, dentin phosphoprotein; DSP, dentin sialoprotein; SIBLING, small integrin-binding ligand *N*-linked glycoprotein; MAP, mitogen-activated protein; BME, basal medium Eagle; ELK, eukaryotic-like protein kinase; TRITC, tetramethylrhodamine isothiocyanate; OCN, osteocalcin; BSP, *bone sialoprotein; OPN,* osteopontin.

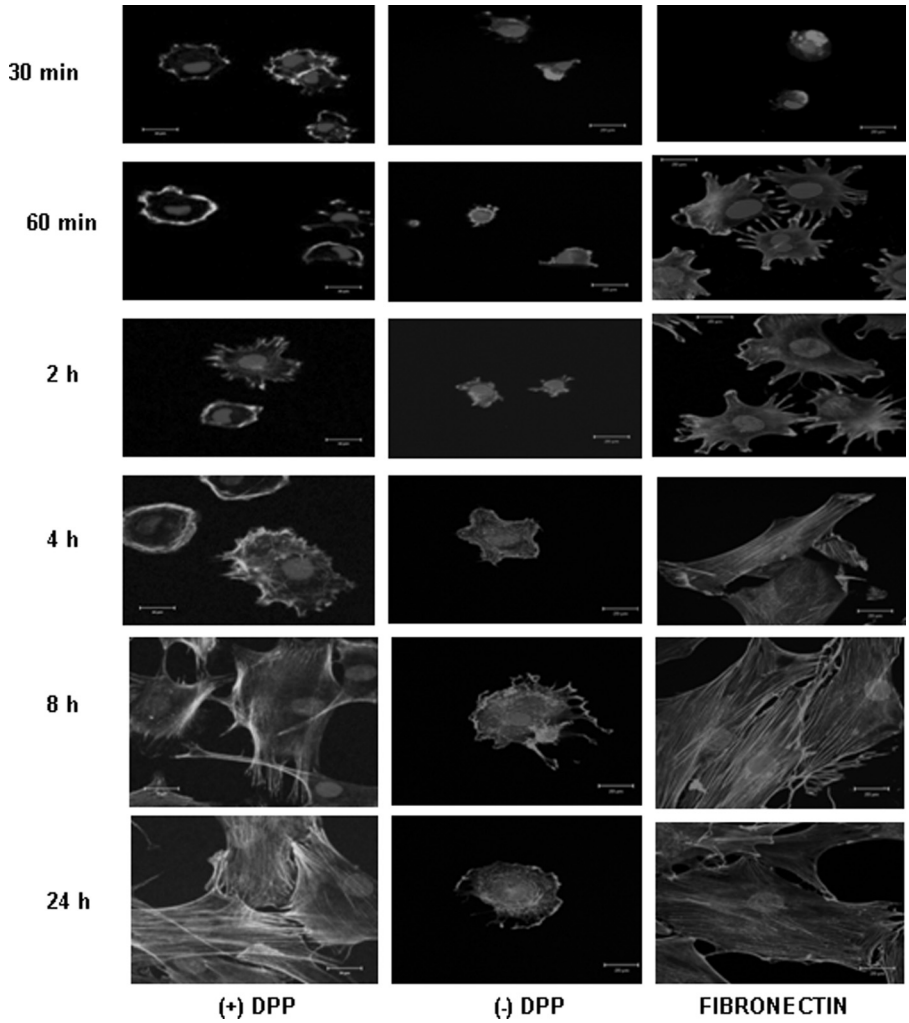

FIGURE 1. **DPP on substrate increases C3H10T1/2 cell spreading and adhesion.** C3H10T1/2 cells were seeded on DPP- or non-DPP-coated (*(−)DPP*) coverglass for 30 min to 24 h. The cells were fixed and stained for actin. Cells seeded on fibronectin served as a positive control. *Scale bars*, 20 μm.

mately impact cell proliferation, differentiation, cell spreading, and migration (28).

However, the RGD-mediated functions of DPP have not been explored. In this report, we investigate the signaling pathway activated by immobilized DPP. We hypothesize that integrins of undifferentiated embryonic mesenchymal stem cells such as C3H10T1/2 and primary dental pulp cells bind to immobilized DPP, and this results in the formation of a multiprotein scaffolding complex and signaling unit. The formation of this complex might promote the activation of signal transduction pathways like the MAP kinase pathway, resulting in cell differentiation.

MATERIALS AND METHODS

Cell Culture—Mouse embryonic mesenchymal (C3H10T1/2) cells were cultured in BME supplemented with 10% FBS and 1% penicillin-streptomycin. Primary dental pulp cells were isolated from day 3 mice and grown in α-minimum Eagle's medium supplemented with FBS and penicillin-streptomycin. 12–16 h before the start of the experiment, the cells were cultured in BME or α-minimum Eagle's medium supplemented with 1% FBS. Non-tissue culture grade 6-well plates were coated with recombinant DPP (750 ng/ml) in carbonate buffer. The cells were rinsed with PBS, trypsinized, and seeded at 80% confluence. C3H10T1/2 cells seeded on 6-well plates coated with carbonate buffer served as control.

DPP Coating on Non-tissue Culture Plates—Non-tissue culture plates coated with DPP were prepared by soaking the plate with 750 ng/ml DPP in 20 mM carbonate buffer, pH 9.3 overnight at 4 °C in a humidified atmosphere for 2 days. Before use, the protein solution was removed, and the plates were rinsed twice in PBS.

Cell Culture Transfections—Transient transfection of ELK plasmid and empty vector (a kind gift from A. Alpin, Albany Medical College, Albany, NY) into C3H10T1/2 cells seeded on DPP-coated plates was performed using Superfect (Qiagen, Valencia, CA). After 48 h of transfection, these cells were stained for ELK. Transfection performed on tissue culture plates followed by staining for ELK served as a positive control. Transient transfection was also performed with mRFPruby-actin (a kind gift from A. Müller-Taubenberger, Ludwig Maximilians University, Munich, Germany) constructs using FuGENE HD (Promega, Madison, WI).

Quantitative Real Time PCR—RNA was extracted according to the manufacturer's recommended protocol by using TRIzol

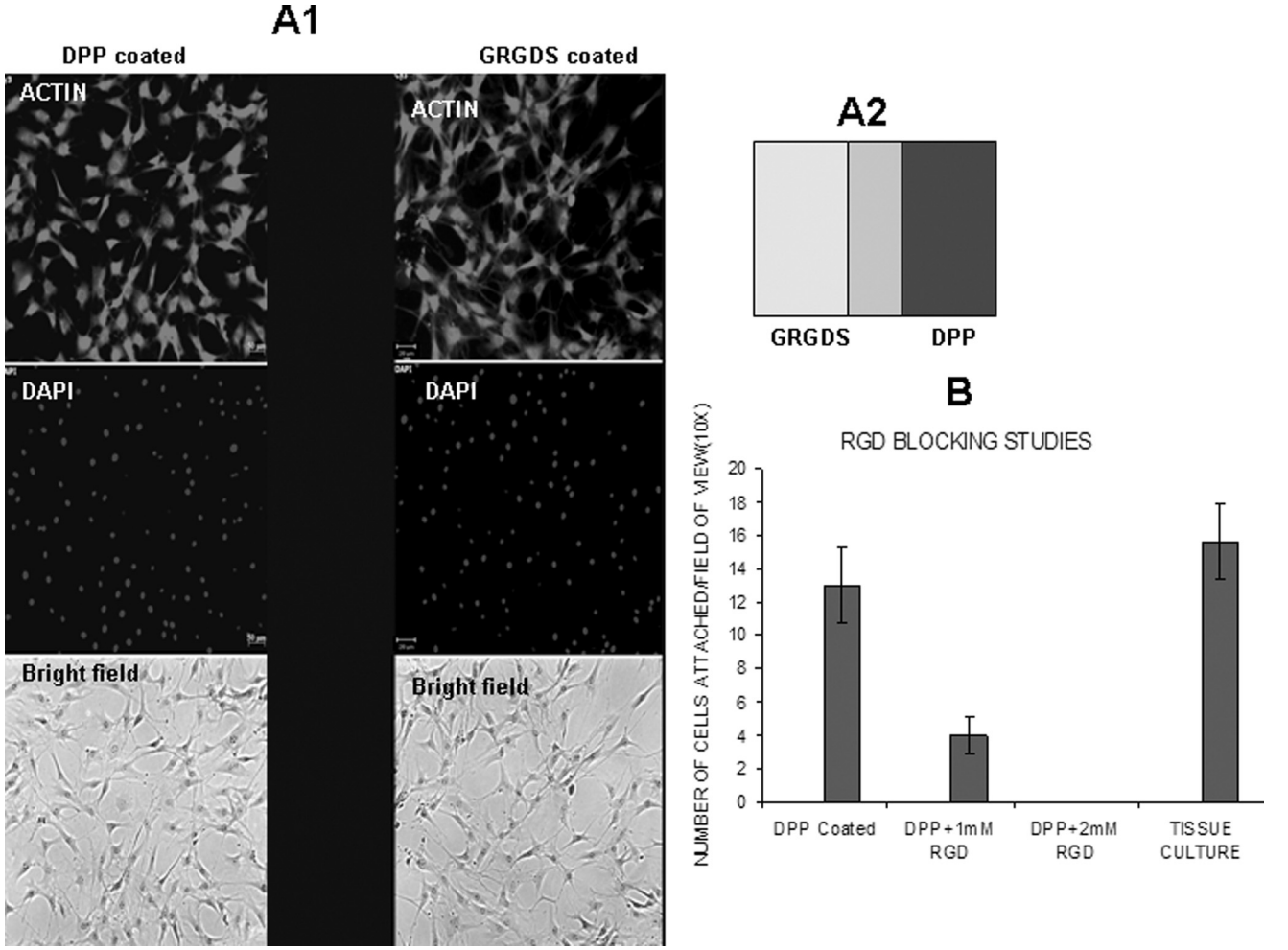

FIGURE 2. **RGD domain in DPP facilitates cell attachment.** Gold substrate was stamped with DPP on one side and an RGD peptide on the other side. C3H10T1/2 cells were seeded on the substrate for 4 h, fixed, and stained with actin (*A1*). The stamping pattern is schematically represented in *A2*. C3H10T1/2 cells were incubated with a 1 or 2 mM concentration of RGD blocking peptide for 2 h. Cells were then allowed to attach on a DPP-coated coverglass and manually counted with a hemocytometer. The bar graph represents the number of attached cells (*B*). *Scale bar*, 50 μm. *Error bars* represent mean ± standard deviation ($n = 3$).

(Invitrogen). RT-quantitative real time PCR was performed with DNase I (Promega)-treated RNA. A total of 1 μg of total RNA was reverse transcribed for 90 min at 50 °C with Superscript III (Invitrogen). After RNA extraction, quantitative real time PCR analysis was carried out using an ABI Step One Plus machine. Expression for *OCN*, *DMP1*, *DSP*, *RUNX2*, *BSP*, *OPN*, *BMP4*, *MMP9*, and *GAPDH* transcripts was analyzed by quantitative real time PCR during its linear phase. The relative gene expression level was estimated by using the $2^{-\Delta\Delta}C_T$ method where the C_T value is the log-linear plot of PCR signal *versus* the cycle number. $\Delta C_T = C_T$ value of target gene $- C_T$ value of GAPDH. Primers were obtained from Qiagen. Supplemental Fig. S1 shows the primer sequences.

Immunofluorescence—Cells were cultured on recombinant DPP-coated non-tissue culture grade glass coverslips for various time points. Cells were fixed in 4% paraformaldehyde, then permeabilized with 0.1% Triton X-100 in PBS for 5 min, and rinsed twice with wash buffer. After blocking for 30 min, the cells were then incubated overnight in primary antibody, namely anti-FAK, anti-paxillin, anti-ELK, and anti-phospho-extracellular signal-regulated kinase (ERK) 1/2, followed by incubation with a Cy3-conjugated secondary antibody for 1 h. After washing the cells three times with PBS, the coverglass was mounted using mounting medium (VECTASHIELD, Vector Laboratories, Burlingame, CA) and visualized with an Axio Observer D1 fluorescence microscope (Zeiss, Thornwood, NY) equipped with Axiovision imaging software (Zeiss). Actin staining (1:100) was done on these cells at different time points followed by DAPI staining for the nucleus.

Western Blot Analysis—Activation of the focal adhesion complex and the MAP kinase pathway was determined by Western blot analysis. Total proteins were extracted from C3H10T1/2 cells grown on DPP-coated plates with or without mineralization medium using M-PER reagent (Pierce). A total of 35 μg of the protein was resolved by 10% SDS-PAGE under reducing conditions. After electrophoresis, the proteins were electrotransferred onto nitrocellulose membrane (Bio-Rad); blocked with 3% BSA in 1× PBS; and probed with either anti-FAK, anti-paxillin, anti-ERK1/2, anti-phospho-FAK, anti-phosphopaxillin, anti-phospho-ERK1/2 (1:500) (Santa Cruz Biotechnology, Santa Cruz, CA), anti-DMP1 (1:500) (20), or anti-DSP (1:2000) (20). HRP-conjugated goat anti-

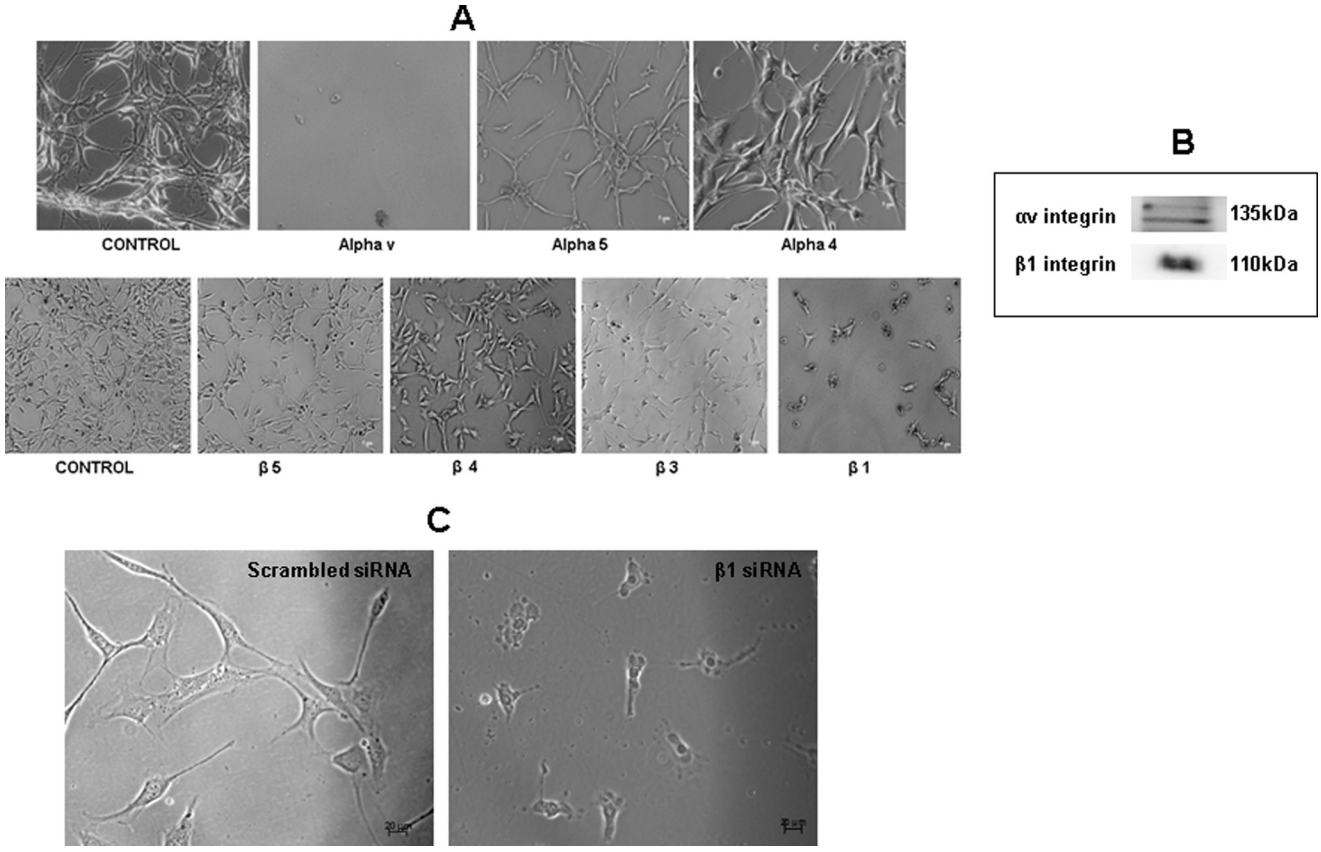

FIGURE 3. **Identification of the cell surface α and β integrins specific for DPP ligand.** Receptor-cell binding experiments were performed by incubating C3H10T1/2 cells with either αv, α4, α5, β5, β4, β3, or β1 antibody for 2 h, respectively. The combinations of cells with the integrin antibodies were seeded on DPP-coated plates and incubated for 24 h. Light microscopic images (Zeiss) of the cells on DPP-coated plates were imaged (*A*). Note the specificity of the αv and β1 antibodies. Specificity was confirmed by isolating membrane proteins, and Western blotting was performed using αv and β1 integrin antibodies (*B*). β1 integrin siRNA transfection was performed in C3H10T1/2 cells grown on DPP-coated plates. 0.5 μg of the siRNA was used for transfection. Transfection performed with scrambled siRNA was used as the control (*C*).

rabbit IgG was used for detection (Chemicon International, Temecula, CA). West pico Chemiluminescent reagent (PerkinElmer Life Sciences) was used as substrate for HRP. Each membrane was then carefully washed, treated for 5 min with a stripping buffer to eliminate the previous reaction (Pierce), washed with PBS, and processed as above with anti-tubulin antibody (1:10,000; Sigma) and HRP-conjugated goat anti-mouse IgG.

Identification of Cell Surface Receptor—1×10^4 C3H10T1/2 cells were preincubated with each of the antibodies for αv, α4, α5, β5, β4, β3 (1:50; Cell Signaling Technology, Danvers, MA), or β1 (a kind gift from S. Carbonetto, McGill University, Montreal, Quebec, Canada) for 2 h on a rotor at 37 °C. Following incubation, the cells were seeded on DPP-coated plates and incubated for 24 h at 37 °C. C3H10T1/2 cells seeded on DPP-coated plates were used as a control. Confocal images (Zeiss) of the cells were taken.

Isolation of Cell Surface Receptor—C3H10T1/2 cells were treated with recombinant GST-DPP (1 mg/ml) for 1 h at 4 °C to ensure binding but not endocytosis. The cells were then washed with ice-cold PBS three times after which the membrane proteins were isolated using Pierce reagent. The membrane proteins were incubated with Sepharose beads overnight at 4 °C. The beads were then washed with PBS containing 150 mM NaCl. The bound proteins were eluted with glutathione, dialyzed against 1 mM Tris, and lyophilized. The lyophilized protein was redissolved in 50 μl of PBS, and immunoblotting was performed with integrin αv antibody (1:500; Cell Signaling Technology) and β1 integrin antibody.

Transient Transfection for β1 Integrin siRNA—C3H10T1/2 cells were grown to 60% confluence on DPP-coated plates and transfected with β1 integrin siRNA (0.5 μg) or scrambled siRNA duplexes (0.5 μg) (Santa Cruz Biotechnology) as a control using siRNA transfection reagent (Santa Cruz Biotechnology). Cell attachment was observed and photographed after 24 h.

Blocking Experiments with RGD Peptide—To confirm the involvement of the RGD domain in mediating cell attachment, 1×10^4 C3H10T1/2 confluent cells/ml were incubated for 1 h with 1 and 2 mM RGD peptide (Gly-Arg-Gly-Asp-Asn-Pro) in BME (Invitrogen) on a rotor at 37 °C in an incubator for 2 h prior to plating them on DPP-coated plates. The cells were allowed to attach for 24 h. The adherent cells were fixed, stained with 0.5% trypan blue, and counted manually. Cells seeded on tissue culture plates were used as a control. The experiments were performed in triplicate, and standard errors of the cell numbers were determined. Proteins were extracted according to the above protocol, and Western blotting was performed.

Preparation of Self-assembled Monolayers—Gold substrates were prepared by evaporating titanium (4 nm) followed by gold

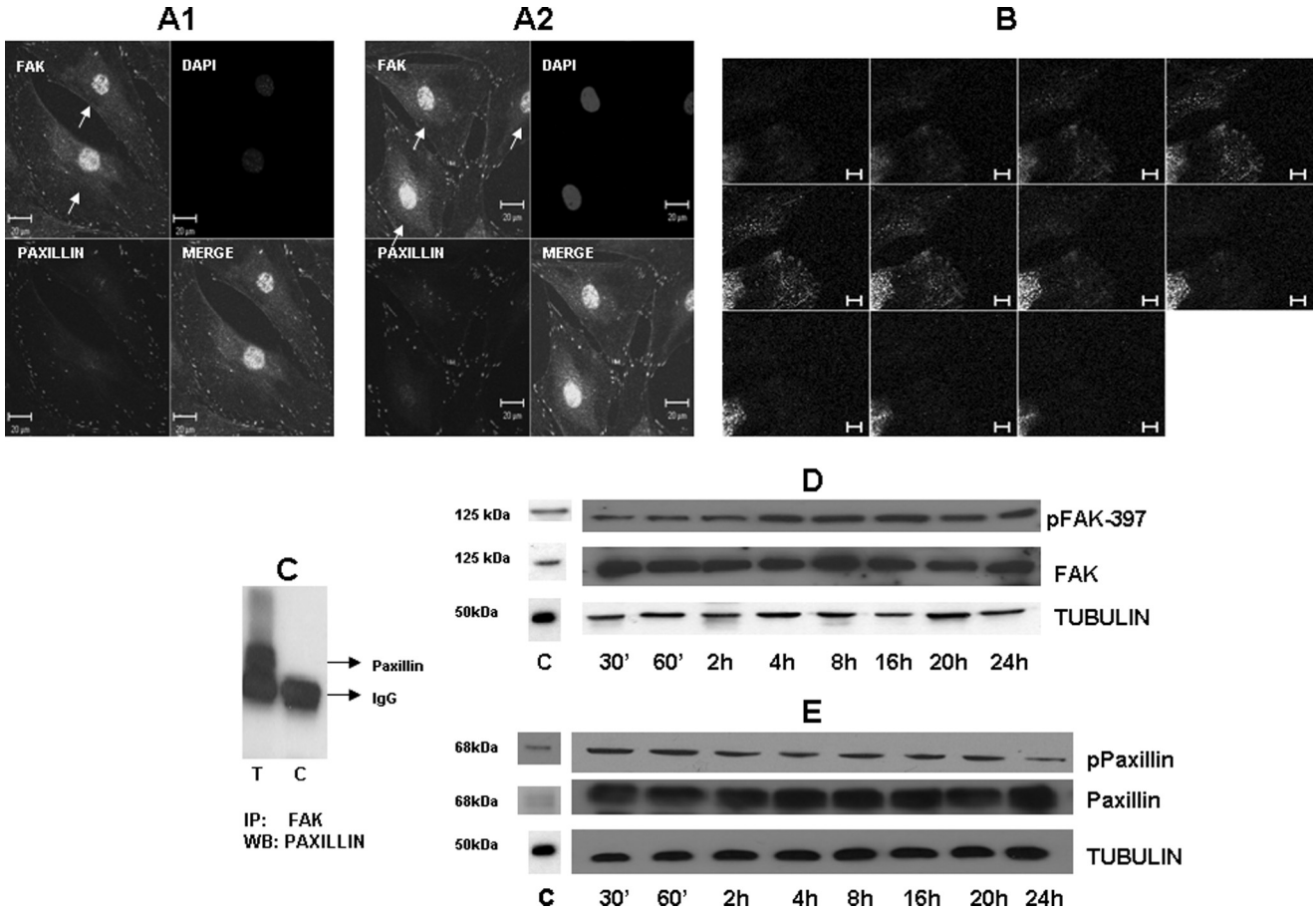

FIGURE 4. **DPP triggers organization of focal adhesion complexes.** C3H10T1/2 cells were seeded on DPP-coated plates for 16 (*A1*) and 24 h (*A2*). Immunohistochemical analysis was performed with paxillin (*red*) and FAK (*green*) antibodies. Confocal microscopic images are presented in *A*. Immunostaining indicates the successful spreading and formation of focal adhesions. FAK is localized at focal adhesions and the nucleus (*single arrows*), whereas paxillin is localized predominantly at focal adhesions. *Scale bars*, 20 μm. Z stack analysis was performed to determine the colocalization of FAK with paxillin at the 24-h time point (*B*). DPP induces *in vivo* association of FAK and paxillin (*C*). "*T*" represents 50 μg of total protein and FAK antibody mixed with protein A beads and incubated overnight. The beads were then washed with PBS, and SDS-PAGE loading dye was added to the beads and boiled. Immunoblot was performed with paxillin antibody. "*C*" represents immunoprecipitation (*IP*) performed in the absence of FAK antibody. C3H10T1/2 cells were seeded on DPP-coated plates, total proteins were isolated at various time points as indicated, and Western blotting (*WB*) was performed to determine activation of FAK (*D*) and paxillin (*E*). Total proteins isolated from C3H10T1/2 cells grown in the absence of DPP were used as a control (*C*). *pPaxillin*, phosphopaxillin; *pFAK*, phospho-FAK; *′*, minutes.

(25 nm) onto glass coverslips using the BOC Edwards Auto 500 system with FL400 chamber (Edwards Ltd., Wilmington, MA). A polydimethylsiloxane stamp with the selected pattern was coated with a solution of 1 mM hexadecanethiol in ethanol. The stamp was then placed on the gold substrate for ~30 s after which they were separated, and the substrate was rinsed with absolute ethanol and dried under a stream of nitrogen. The hexadecanethiol-coated substrate was then immersed overnight in an ethanolic solution of maleimide-terminated disulfides mixed with tri(ethylene glycol)-terminated disulfide in a ratio of 1:99 (final concentration of disulfide was 1 mM) to coat the areas surrounding the hexadecanethiol islands. A polydimethylsiloxane cylinder (inner diameter, 130 mm; outer diameter, 220 mm; height, 150 mm) was placed on the monolayer substrate. The monolayers were then treated with a 1 mM solution of RGD peptide (in 1× PBS, pH 7.4) for 30 min followed by immersion in DPP solution (1 μg/ml in 1× PBS, pH 7.4) overnight. The substrates were rinsed with absolute ethanol and dried under a stream of nitrogen between all steps and solution changes. C3H10-T1/2 cells were then seeded on the substrate at a cell density of 500,000 cells/substrate and allowed to attach for 4 h in a 37 °C incubator with 5% CO_2. After cell attachment, the substrate was rinsed thrice with serum-free medium to remove the unattached cells and observed under a microscope to check for cell attachment on the pattern. The medium was changed to BME containing 0.5% FBS, and cells were left overnight in a cell culture incubator. Cells were then fixed and stained with actin and DAPI.

Inhibition of ERK1/2—Cells were cultured as described above and treated with 30 μM PD98059 inhibitor (Biomol), a specific inhibitor for the ERK1/2 MAP kinase pathway. Cell lysates were harvested at 4- and 24-h time points, and Western blotting and immunofluorescence were performed as described above with anti-ERK1/2 antibody and anti-phospho-ERK1/2 antibody.

Immunoprecipitation—FAK antibody was mixed with protein A beads and incubated on a shaker for 2 h. 50 μg of total protein from C3H10T1/2 cells grown on DPP-coated plates were mixed with the beads and incubated overnight. The beads

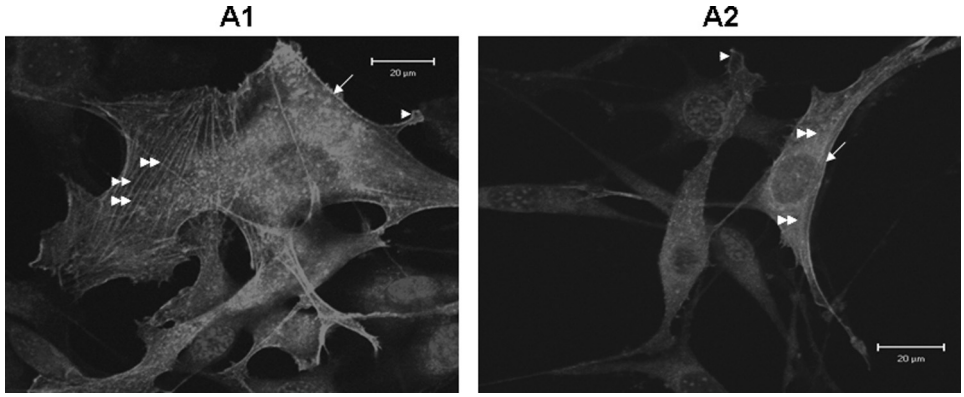

FIGURE 5. **Cells on DPP substrate promote actin polymerization.** C3H10T1/2 cells were transfected with an mRFPruby-actin plasmid using FuGENE HD. The cells were then trypsinized and seeded on a DPP-coated coverglass. Confocal microscopic images were taken at 8 (*A1*) and 24 h (*A2*). Note the incorporation of the mRFPruby-actin into subcompartments of the actin cytoskeleton such as lamellipodium (*single arrows*), filopodia (*single arrowheads*), and stress fibers (*double arrowheads*). *Scale bars*, 20 μm.

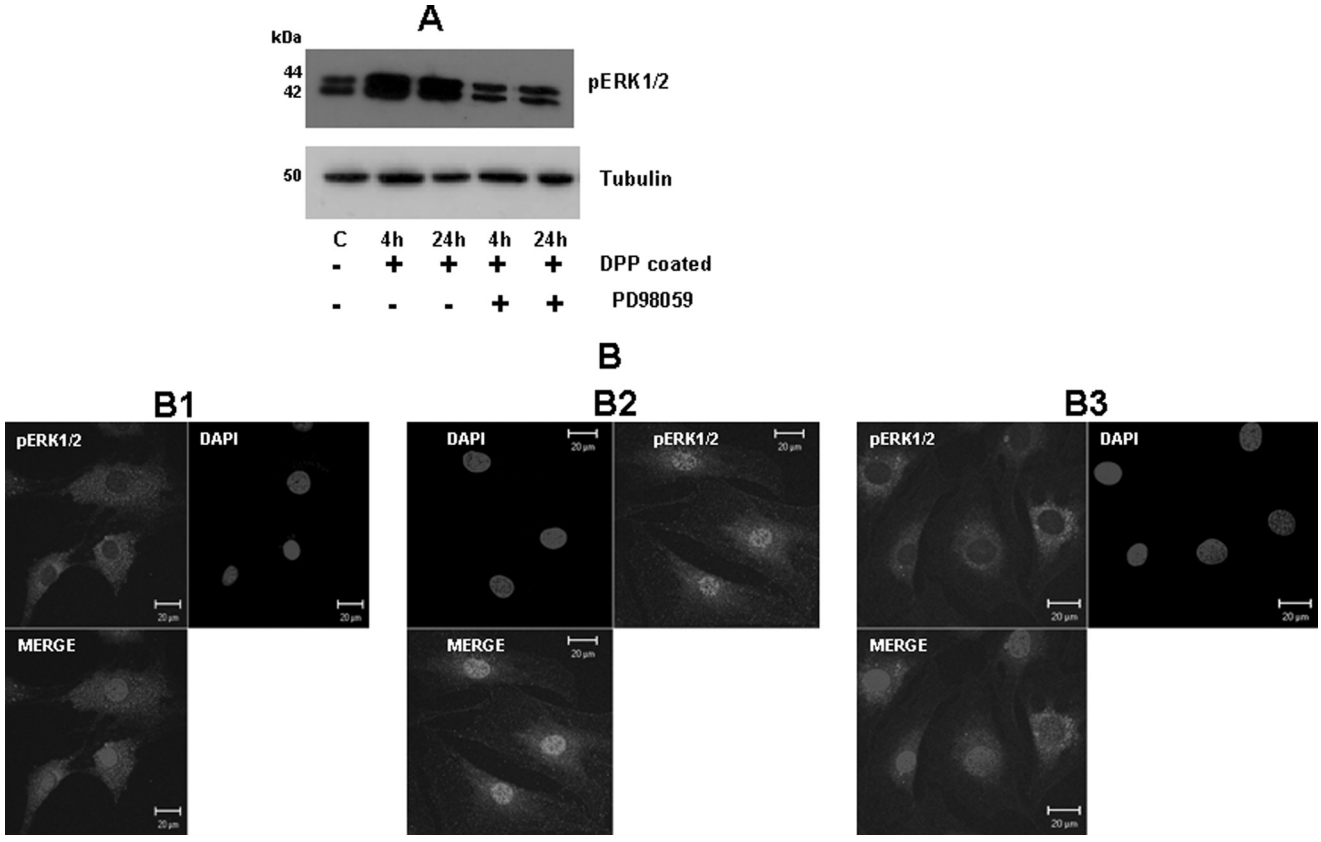

FIGURE 6. **Activation of ERK1/2 MAPK pathway by adherent cells on DPP substrate.** C3H10T1/2 cells were seeded on DPP-coated plates and treated with or without PD98059 for 4 and 24 h. Total proteins were isolated, and Western blotting was performed using phospho-ERK1/2 (*pERK1/2*) and tubulin antibodies. Cells in suspension were used as a control (*A*). Confocal imaging was performed on adherent cells at 24 h. No nuclear localization was observed in cells seeded on tissue culture coverglass (*B1*). Nuclear localization of phospho-ERK1/2 was seen in cells plated on DPP-coated coverglass (*B2*), and this was inhibited after PD98059 treatment for 24 h (*B3*). *C*, control. *Scale bars*, 20 μm.

were then washed three times in 1× PBS to remove nonspecific binding. SDS-PAGE loading dye was added to the beads and boiled for 5 min. The supernatant was resolved on a 10% SDS gel and immunoblotted with paxillin antibody. Immunoprecipitation performed in the absence of FAK antibody served as control.

In Vitro Assay to Determine Differentiation of Mesenchymal Cells to Terminally Differentiated Odontoblast-like Cells—A mineralization microenvironment was induced by the addition of 10 mM β-glycerophosphate and 100 μg/ml ascorbic acid (Sigma-Aldrich) along with 10 nM dexamethasone (Sigma-Aldrich) in the growth medium. Total RNA and total proteins were extracted at 7, 14, and 21 days from C3H10T1/2 cells grown on DPP-coated plates.

von Kossa Staining for Phosphates in Mineralized Nodule—von Kossa staining was performed to determine the presence of phosphate in the mineralized nodules. C3H10T1/2 cells were grown to 60% confluence on DPP-coated plates, and the growth medium was then replaced with mineralization medium for 7, 14, and 21 days. The cells were fixed in for-

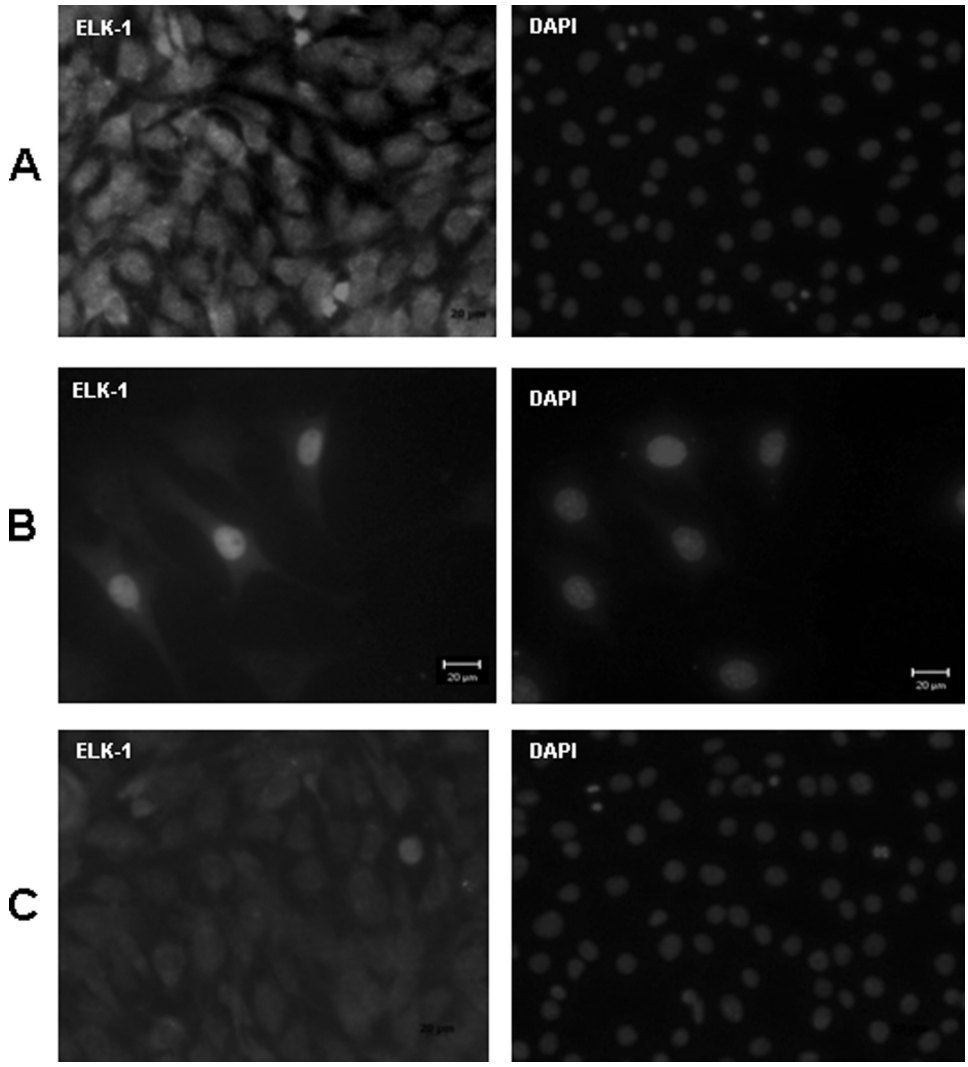

FIGURE 7. **Cells adherent on DPP stimulate nuclear accumulation of ELK-1 transcription factor.** A confocal image of ELK-1 immunostaining performed on C3H10T1/2 cells seeded on DPP-coated coverglass is shown in *A*. A transient transfection of a FLAG construct of ELK-1 was performed using Superfect reagent on C3H10T1/2 cells seeded on DPP-coated plates. Localization of ELK-1 was determined by immunofluorescence with an ELK-1 antibody and TRITC-conjugated anti-rabbit secondary antibody. Nuclear localization of ELK-1 is seen in the DPP-treated plates (*B*). Cells seeded on a tissue culture plate were used as a control (*C*). *Scale bars*, 20 μm.

malin for 20 min, washed twice with distilled water, then stained with 1% silver nitrate solution (Sigma-Aldrich) for 30 min, and photographed. Cells grown on DPP-coated plates without mineralization medium and cells grown on tissue culture plates with mineralization medium were used as controls.

Alizarin Red S Staining for Calcium in Mineralized Nodule—C3H10T1/2 cells were grown to 60% confluence on DPP-coated plates. The growth medium was replaced with mineralization medium for 7, 14, and 21 days. The cells were fixed in formalin for 20 min at room temperature and washed with distilled water. 2% Alizarin Red solution was added to fixed cells and incubated for 10–20 min. The cells were then rinsed with distilled water and imaged.

RESULTS

DPP Aids in Cell Attachment and Cytoskeletal Organization—C3H10T1/2 cells were seeded on DPP-coated non-tissue culture coverglass and cultured for various time points from 30 min to 24 h. The cells were then fixed and stained for actin. Assessment of the attached cells by confocal microscopy (Fig. 1) on DPP-coated substrate show distinct cell responses such as cell spreading as indicated by their F-actin cytoskeletal structure, formation of multiple filopodia, and protrusions of the lamellipodia, whereas cells on non-DPP-coated plates were round and showed no spreading. A coverslip coated with fibronectin served as a positive control (Fig. 1).

Specificity of RGD Domain in Cell Attachment—To define the role of the RGD domain in cell adhesion, glass slides coated with gold substrate stamped with DPP on one-half and GRGDS peptide on the other half with an uncoated region in the middle were used as substrates for the cell attachment assay (Fig. 2). A schematic representation of the stamp containing the two peptides is shown in Fig. 2, *A2*. C3H10T1/2 cells were seeded on the substrate for 24 h, fixed, and stained with actin. The absence of cell adhesion was seen in the center unstamped section of the substrate (Fig. 2, *A1*). Interestingly, cell adhesion looked robust on both the DPP- and GRGDS-stamped surface.

DPP Activates Anchorage-dependent Signals

Cell Adhesion Is Abrogated in Presence of RGD Blocking Peptide—To confirm the involvement of the RGD domain in mediating cell attachment, C3H10T1/2 cells were incubated with a 1 or 2 mM concentration of GRGDS blocking peptide. Cells were then allowed to attach on a DPP-coated coverslip for 24 h. The cells were counted, and we observed that 1 and 2 mM concentrations of the peptide inhibited cell adhesion when compared with the cells without peptide incubation seeded on a DPP-coated plate. Results in Fig. 2*B* showed that a 2 mM concentration of GRGDS peptide showed 100% inhibition on cell attachment when compared with a 1 mM concentration.

Identification and Isolation of Integrin Receptors—The integrin receptors specific for binding of C3H10T1/2 cells to DPP were identified by using a panel of α and β integrin antibodies. When C3H10T1/2 cells were incubated with either αv, α4, α5, β5, β4, β3, or β1 antibody for 2 h and then cultured on DPP-coated plates for 24 h, we observed that the anti-αv and -β1 antibodies abrogated cell adhesion (Fig. 3*A*).

Having identified the cell surface receptor as $\alpha v\beta 1$ integrin, we isolated the cell membrane proteins and performed Western blot analysis for further confirmation. Results in Fig. 3*B* confirmed the presence of $\alpha v\beta 1$ integrins. Knockdown of β1 integrin in C3H10T1/2 cells performed on a DPP-coated plate led to a change in morphology within 4 h, and by 24 h, cells were rounded up and seemed to be undergoing apoptosis (Fig. 3*C*). Thus, $\alpha v\beta 1$ integrin is necessary for the attachment and survival of C3H10T1/2 cells on DPP substrate.

DPP Facilitates Adhesion-mediated Signaling Events by Organization of Focal Adhesions—We next examined the effects of integrin activation on the regulation of FAK and paxillin. We hypothesized that adhesion of C3H10T1/2 cells or primary dental pulp cells to DPP substrate would induce association of FAK and paxillin. Immunohistochemical analysis indicated that FAK and paxillin were expressed on the cell membrane of adherent primary dental pulp cells (supplemental Fig. S2, A and B) and C3H10T1/2 cells at 16 (Fig. 4, *A1*) and 24 h (Fig. 4, *A2*), thereby inducing focal adhesion formation and cell spreading. "Z" stack analysis performed on images obtained at the 24-h time point show clear colocalization of FAK with paxillin (Fig. 4*B*). Signaling molecules participating in a pathway are usually in a direct physical association, and immunoprecipitation analysis confirmed the *in vivo* association of FAK and paxillin in C3H10T1/2 cells (Fig. 4*C*). Importantly, we observed the nuclear translocation of FAK on cells adherent to DPP substrate at 16- and 24-h time points. FAK is a 125-kDa protein that is tyrosine phosphorylated and activated in response to integrin clustering. Western blot analysis (Fig. 4*D*) confirmed FAK activation as Tyr^{397} is phosphorylated. This initial phosphorylation is necessary for tyrosine phosphorylation of multiple sites in FAK and paxillin. Results in Fig. 4*E* show activation of paxillin in C3H10T1/2 cells seeded on DPP-coated plates from 30 min to 24 h. Cells plated on carbonate buffer-coated slides did not show colocalization of FAK and paxillin at focal adhesions (data not shown).

DPP Regulates Actin Assembly—Actin polymerization drives the extension of sheetlike (lamellipodia) and rodlike protrusions (filopodia) at the cell front. Therefore, to visualize the actin cytoskeleton, C3H10T1/2 cells were transfected with mRFPruby-actin plasmid and replated on DPP substrate. Fluorescence images in Fig. 5 suggested that ectopically expressed mRFPruby-actin was copolymerized with endogenous actin as shown at 8 (Fig. 5, *A1*) and 24 h (Fig. 5, *A2*). Incorporation of mRFPruby-actin was clearly observed in the subcompartments of the actin cytoskeleton such as microspikes, lamellipodium, filopodium, and contractile bundles. Thus, protein assemblies are recruited to the tips of lamellipodia and filopodia that drive the polymerization of actin for protrusion when cells are plated on DPP matrix. It is this actin assembly that generates mechanical signals, transduces them into intracellular signals, and favors gene expression.

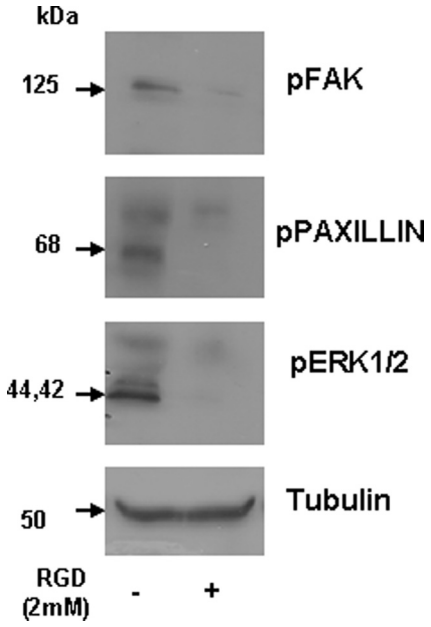

FIGURE 8. **Blocking RGD abrogates activation of FAK, paxillin, and ERK1/2.** C3H10T1/2 cells were incubated with 2 mM RGD peptide at room temperature for 2 h. The cells were then seeded on DPP-coated plates. Total protein was isolated after 24 h, and immunoblotting was performed with anti-phospho-ERK1/2 (*pERK-1/2*), phospho-FAK (*pFAK*), phosphopaxillin (*pPaxillin*), and tubulin antibodies. Cells seeded on a DPP-coated plate were used as a control.

DPP Activates MAP Kinase Signaling—MAP kinases are used by cells to transduce signals from the extracellular environment to the nucleus, ultimately resulting in cell proliferation, differentiation, and survival. It has been shown that activation of the ERK could be controlled by adhesion via integrins (29). To investigate whether adherent cells on DPP substrate induced ERK phosphorylation, we performed Western blot analysis, which showed an increase in phosphorylation of ERK1/2 at 4- and 24-h time points (Fig. 6*A*). Interestingly, this activation was suppressed in the presence of the ERK-specific inhibitor PD98059. Cells on tissue culture plates were used as control (Fig. 6*A*).

Next we sought to analyze the role of adhesion upon the localization of phospho-ERK. By confocal analysis, we determined that in DPP-mediated adherent cells phospho-ERK was localized primarily in the nuclear compartment (Fig. 6, *B2*) and predominantly cytoplasmic in cells plated on tissue culture plates (Fig. 6, *B1*). We then studied the specificity of this activation by using PD98059, a pharmacological inhibitor specific

for the ERK1/2 pathway. PD98059 treatment for 24 h abrogated the translocation of phospho-ERK1/2 into the nucleus (Fig. 6, *B3*). Nuclear localization of phospho-ERK1/2 was also observed when primary dental pulp cells were plated on DPP-coated plates (supplemental Fig. S2C).

DPP Activates ELK-1, a Downstream Target of ERK Signaling—Having established that translocation of ERK to the nucleus is regulated by cell adhesion to the DPP substrate, we next analyzed whether ELK-1 is a substrate for activated ERK. ELK-1, a transcription factor, is a known substrate of ERK, and phosphorylation at the C-terminal site is important for its transcriptional activity (30). To this end, we expressed a construct (pCMV5-FLAG-ELK-1) in C3H10T1/2 cells seeded on DPP-coated plates as low levels of endogenous ELK-1 are expressed by these cells. Results in Fig. 7 show clear nuclear localization of ELK-1 on DPP-treated plates. As expected, cells seeded on a tissue culture plate did not result in nuclear translocation of ELK-1 (Fig. 7). Interestingly, nuclear localization of ELK-1 was observed when primary dental pulp cells were plated on DPP-coated plates (supplemental Fig. S2D). Together, these results suggest that activation of ELK-1 is adhesion-dependent in response to DPP that correlates with ERK1/2 activation.

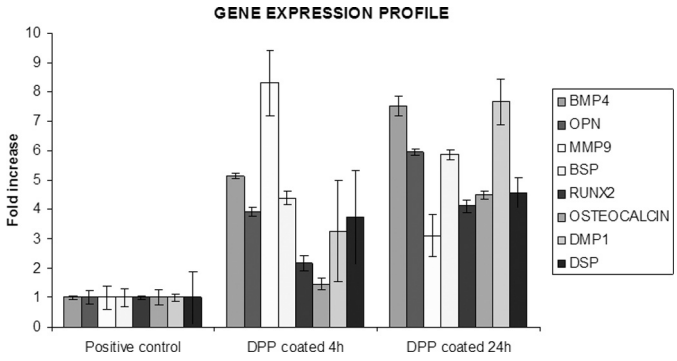

FIGURE 9. **DPP induces odontogenic differentiation in C3H10T1/2 cells.** C3H10T1/2 cells were seeded on DPP-coated plates for 4 and 24 h. Total RNA was isolated, subjected to real time PCR, and analyzed for the expression of *RUNX2*, *DSP*, *DMP1*, *BMP4*, *BSP*, *OPN*, *MMP9*, and osteocalcin (*OCN*). *Error bars* represent mean ± standard deviation ($n = 3$). GAPDH was used as the housekeeping gene.

Blocking RGD Inhibits Activation of FAK, Paxillin, and ERK1/2—To confirm that the biological ramifications that we observed, namely activation of FAK, paxillin, and ERK1/2, were in response to the RGD domain in DPP, we used a blocking peptide to the RGD domain to study its role in signaling and attachment. As before, we were able to see an activation of FAK, ERK1/2, and paxillin in cells on DPP-coated plates. Importantly, this activation was inhibited in the presence of a 2 mM concentration of the blocking RGD peptide (Fig. 8). Taken together, these data show that RGD in DPP plays a pivotal role in the activation of the adhesion complex, which in turn leads to the activation of the MAP kinase signaling pathway, leading to cellular differentiation.

Attachment of C3H10T1/2 Cells on DPP Matrix Triggers Odontogenic Differentiation—Odontogenic differentiation of C3H10T1/2 on DPP-coated plates was demonstrated by an increase in the relative expression of markers like *DSP*, *DMP1*, *RUNX2*, *BMP4*, osteocalcin (*OCN*), *OPN*, and *BSP* at 4 and 24 h after attachment. However, these markers remained unchanged for cells that were seeded on tissue culture plates (positive control) (Fig. 9). Most interestingly, we observed an increase in the expression of matrix metalloprotease 9 at 4 h

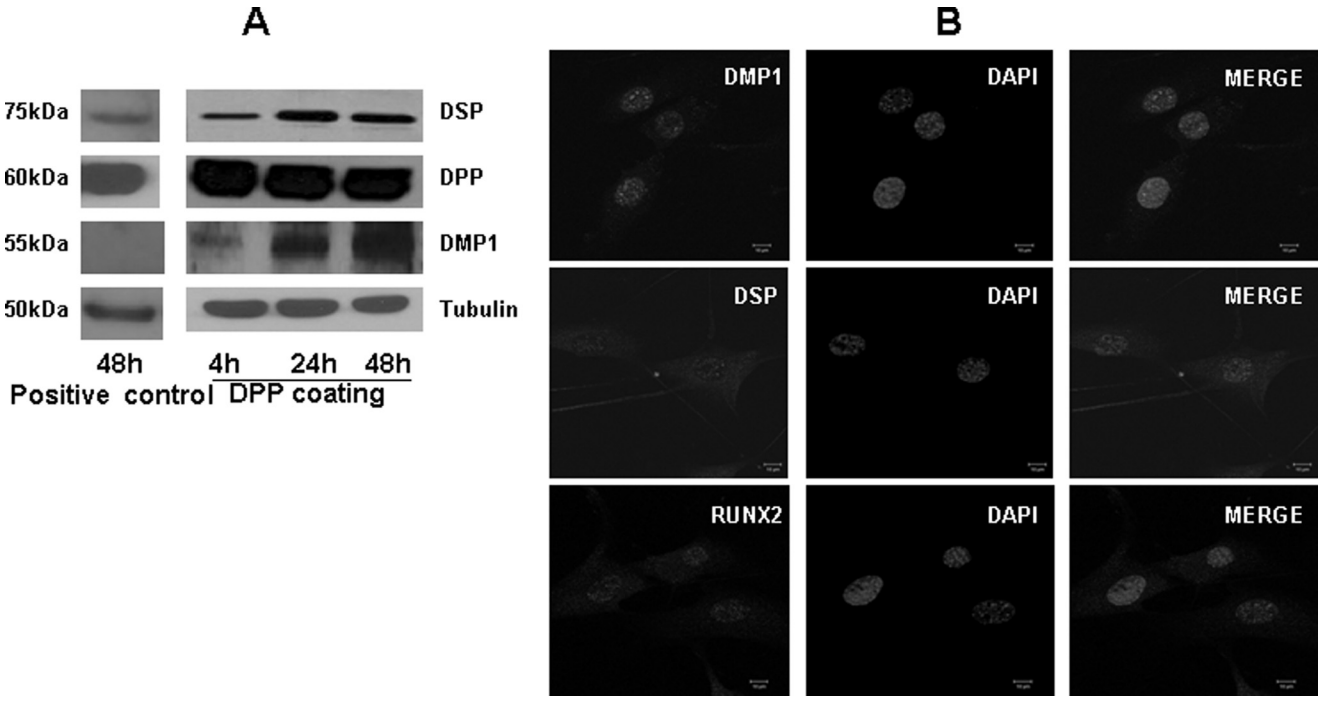

FIGURE 10. **DPP triggers nuclear localization and protein synthesis of odontogenic markers of differentiation.** Total protein was isolated from cells seeded on DPP-coated plates at 4, 24, and 48 h, and immunoblotting was performed with DMP1, DSP, DPP, and tubulin antibodies (*A*). Cells seeded on a tissue culture plate for 48 h were used as a control. A confocal image of C3H10T1/2 cells seeded on DPP-coated coverglass for 24 h and immunostained using antibodies for DSP, DMP1, and RUNX2 is shown (*B*). Nuclear localization of DSP, DMP1, and RUNX2 was seen in cells plated on DPP-coated coverglass. *+ve*, positive; *pERK1/2*, phospho-ERK1/2.

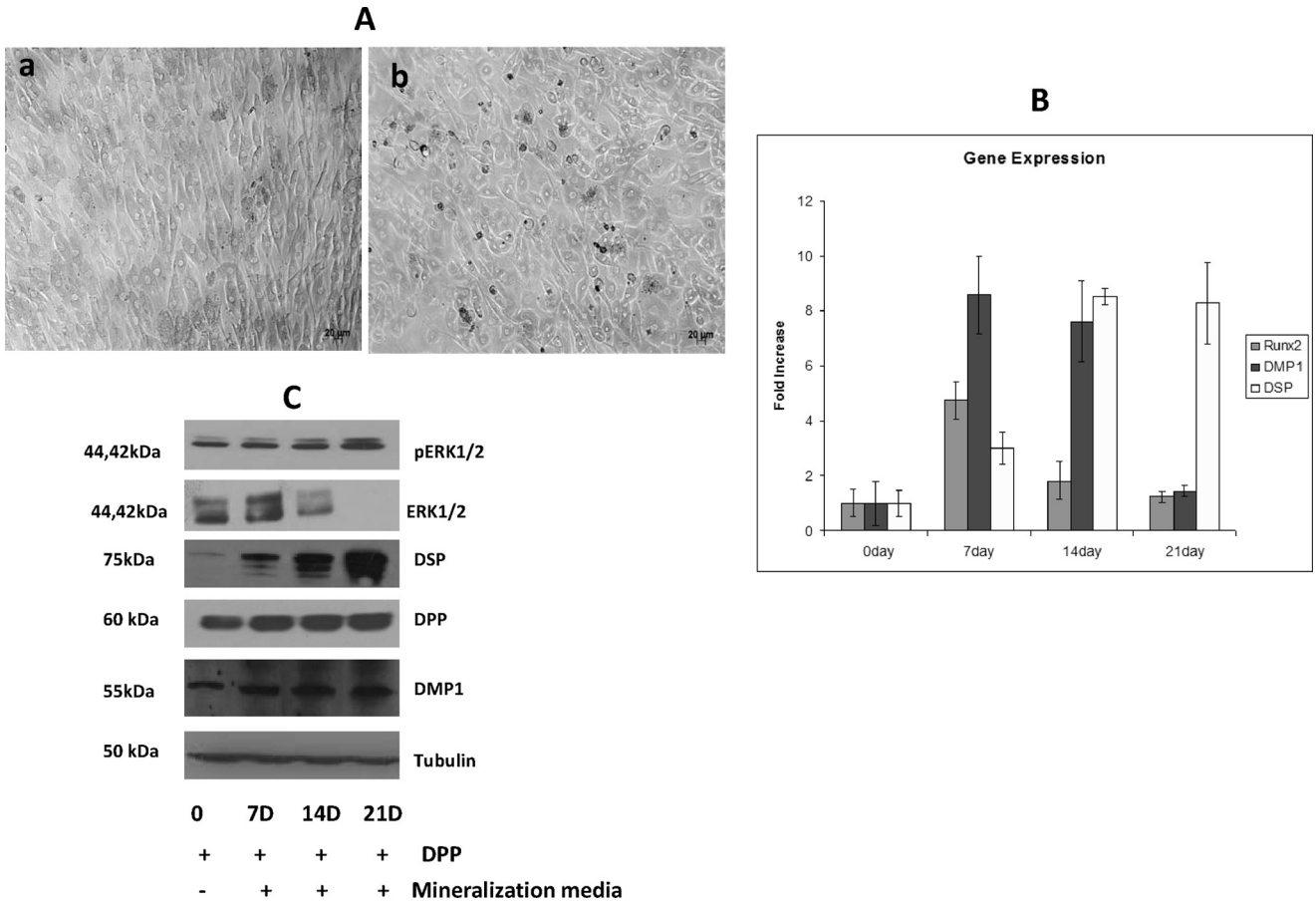

FIGURE 11. **DPP plays important role in terminal differentiation of odontoblast.** C3H10T1/2 cells seeded on DPP-coated plates were grown in mineralization medium for 7, 14, and 21 days. Light microscopic images of the cells in the presence and absence of mineralization medium at 21 days were taken (*A*). Changes in the morphology of the cells were observed in the absence (*A*, *panel a*) and presence (*A*, *panel b*) of mineralization medium. *Scale bars*, 20 μm. RNA was extracted using TRIzol at 7, 14, and 21 days, and real time PCR was performed for *RUNX2*, *DSP*, and *DMP1* (*B*). Total proteins were isolated from C3H10T1/2 cells seeded on DPP-coated plates and grown under mineralization conditions for 7, 14, and 21 days (*C*). Immunoblotting was performed with DSP, DMP1, DPP, and phospho-ERK1/2 (*pERK1/2*). Total proteins isolated from cells grown on DPP-coated plates for 21 days in the absence of mineralization medium were used as control. *Error bars* represent mean ± standard deviation.

when compared with the 24-h time point, suggesting a role for *MMP9* in DPP-mediated cellular differentiation.

DPP Stimulates Expression and Nuclear Translocation of Differentiation Markers—Western blot analysis performed on cells grown on DPP-coated plates at 4, 24, and 48 h showed up-regulation for DSP, DMP1, and DPP (Fig. 10*A*) as compared with the controls obtained from tissue culture plates at 48 h. We next explored the subcellular localization of the odontogenic markers DSP, DMP1, and RUNX2 in C3H10T1/2 cells undergoing differentiation. Immunohistochemical staining showed nuclear localization of DSP, DMP1, and RUNX2 (Fig. 10*B*).

DPP Promotes Terminal Differentiation of Undifferentiated Mesenchymal Cells—To detect morphological changes during odontogenic differentiation, C3H10T1/2 cells seeded on DPP-coated plates were subjected to mineralization for 7, 14, and 21 days, and light microscopic images were obtained. Cells in the presence of mineralization medium at 21 days clearly show a change in the morphology of the cells from cobble-shaped to spindle-shaped (Fig. 11*A*, *panel a*) to cellular clustering during mineralization when compared with the control (Fig. 11*A*, *panel b*). Changes in cellular morphology were also correlated with changes in odontogenic gene expression. mRNA expression for *RUNX2*, *DSP*, and *DMP1* was assessed at time points ranging from 7 to 21 days (Fig. 11*B*). An initial significant increase in the *RUNX2* gene expression was observed at 7 days, indicating an early role for *RUNX2* in the odontogenic differentiation program. The mRNA levels of DMP1 were observed to be significantly up-regulated at 7 and 14 days and down-regulated at 21 days. Interestingly, elevated DSP gene expression was detected at all time points using real time PCR.

Western blots were also performed on total proteins isolated from C3H10T1/2 cells seeded on DPP-coated plates grown under the mineralization condition for 7, 14, and 21 days. Immunoblots showed a significant increase in DSP, DMP1, DPP, and phospho-ERK1/2 expression from day 7 to day 21 when compared with the control cells, which were obtained at 21 days in the absence of differentiation medium (Fig. 11*C*).

DPP Stimulates Mineralized Nodule Formation in C3H10T1/2 Cells—To provide evidence that DPP supports the progression of odontoblast differentiation, von Kossa staining was performed at time points 7, 14, and 21 days (Fig. 12*A*). Odontogenic differentiation and mineralization were observed at all times points on DPP-coated plates. At 14 and 21 days of culture, von Kossa staining showed dark deposits in the extracellular matrix, demonstrating the presence of phosphate in the calcified nodules. In contrast, cells grown on

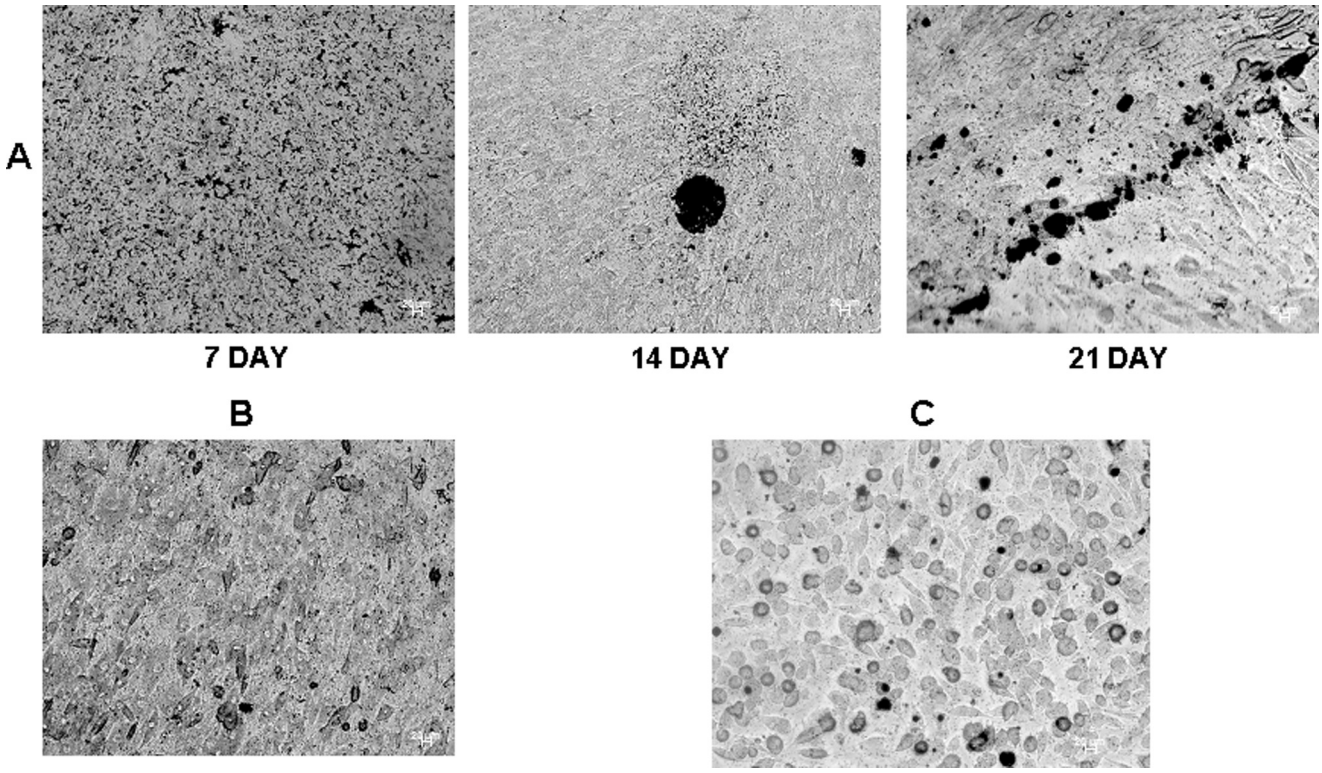

FIGURE 12. **DPP triggers mineralized nodule formation in C3H10T1/2 cells.** von Kossa staining was performed on C3H10T1/2 cells seeded on DPP-coated plates grown in mineralization medium for 7, 14, and 21 days (*A*). The cells were fixed in formalin, washed twice with distilled water, and then stained with 1% silver nitrate solution. von Kossa staining demonstrated a high intensity of dark staining pattern at 14 and 21 days of culture. Cells grown on DPP-coated plates without mineralization medium (*B*) and cells on a tissue culture plate with mineralization medium (*C*) were used as controls. *Scale bars*, 20 μm.

DPP-coated plates in the absence of mineralization for 21 days showed no staining (Fig. 12*B*). C3H10T1/2 cells grown on a tissue culture plate with mineralization medium served as a control (Fig. 12*C*).

Odontogenic terminal differentiation of C3H10T1/2 cells was further confirmed by Alizarin Red staining. C3H10T1/2 cells seeded on DPP-coated plates grown in the presence of mineralization medium for 14 and 21 days resulted in staining of the mineralized matrix, demonstrating the presence of calcium deposits (Fig. 13*A*). Interestingly, no such staining was detected when cells were grown in mineralization conditions on tissue culture plates for 7, 14, and 21 days (Fig. 13*B*).

DISCUSSION

Living cells grow and function while tightly associated with the diverse connective tissue components that form the extracellular matrix (31). The extracellular matrix comprises a scaffold on which tissues are organized, provides biological cues, and regulates multiple cellular functions. Furthermore, the rigidity of the extracellular environment controls the differentiation of the mesenchymal stem cells (32) and the self-renewal of hematopoietic stem cells (33). The integrins are a large family of cell adhesion receptors, which mediate cell-cell and cell-matrix adhesion (34). Their functions have been implicated in processes like development, immune response, and maintenance of tissue integrity, whereas in pathological conditions, they participate in chronic inflammation, invasion of cancer cells, and metastasis (35). Major extracellular matrix proteins such as fibronectin and collagen bind to several integrins (36, 37). During tooth development, odontoblasts arise from neural crest-derived undifferentiated ectomesenchymal cells and undergo sequential steps of differentiation, and integrins play an important role in this process (38).

This study describes the cooperative effects between DPP and $\alpha v\beta 1$ integrin that result in anchorage of undifferentiated embryonic mesenchymal cells. Knockdown of $\beta 1$ integrin confirmed the central role of $\beta 1$ integrin in cell attachment. Binding of cell-specific integrins to DPP substrate can have substantial effects on gene expression by influencing signaling processes. We report that the RGD present at the N terminus of DPP plays a specific role in adhesion. Blocking of the RGD binding site present on the cell surface with a peptide resulted in impaired adhesion and differentiation.

The effect of DPP-mediated adhesion on the activation of FAK, a cytoplasmic protein tyrosine kinase that has been implicated in integrin-mediated signal transduction, was studied. Results from this study show that cells adherent to DPP substrate had increased FAK phosphorylation. This phosphorylation was most pronounced in cells adherent at 4, 8, and 16 h. Tyr^{397} is a major autophosphorylation site in FAK that functions as a binding site for Src homology 2-containing proteins in the adhesion complex (39, 40). Interestingly, phospho-FAK was also localized in the nucleus. The role of nuclear FAK in the cellular differentiation process is currently unclear; however, a recent study has shown that nuclear FAK targets p53 for degradation and enhances cell survival and differentiation (41).

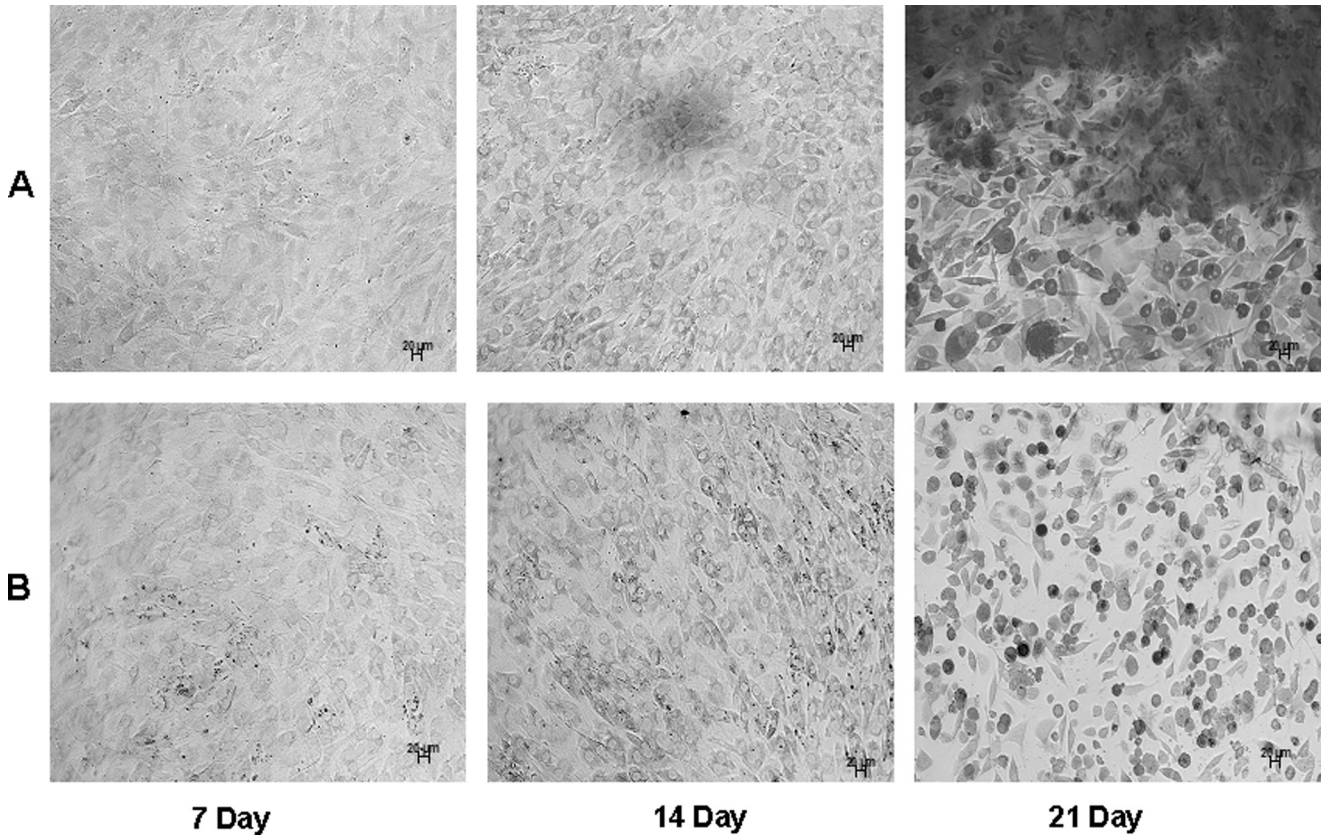

FIGURE 13. **DPP induces matrix mineralization in C3H10T1/2 cells.** C3H10T1/2 cells seeded on DPP-coated plates were grown in the presence of mineralization medium for 7, 14, and 21 days (*A*). Matrix mineralization is indicated by the *dark* areas as a result of calcium staining with Alizarin Red. As controls, cells were grown in mineralization conditions on tissue culture plates for 7, 14, and 21 days (*B*). *Scale bars*, 20 μm.

Thus, nuclear localization of FAK in cells attached to DPP substrate might indicate the activation of cell differentiation pathways.

Binding of integrin receptor to DPP substrate should facilitate the recruitment of signaling molecules to the focal adhesion site. Therefore, we examined the focal adhesion complex protein paxillin as it is a substrate for FAK-containing adhesion complex (42, 43). Upon cell adhesion, we observed phosphorylation of paxillin. Paxillin is a key scaffolding protein between the focal adhesion complex and the actin cytoskeleton that is known to bind to FAK and mediate FAK recruitment to focal adhesion complexes and that is tyrosine phosphorylated by FAK and/or Src in response to integrin engagement (44). Paxillin immunoblots of endogenous FAK precipitates demonstrated *in vivo* association of FAK and paxillin in the complex. The subcellular localization of DPP-mediated FAK-paxillin association showed that paxillin was distributed in discreet focal adhesions at the cell periphery, whereas FAK was distributed both in the nucleus and at the cell periphery. In particular, focal adhesion complexes appeared to condense at the leading edges of the cell processes with FAK-paxillin colocalization at these sites.

The integrin-mediated adhesions are multiprotein complexes that link the extracellular matrix to the actin skeleton (31, 45). Cells on DPP substrate show distinct actin organization with *de novo* formed actin-rich lamellipodium with prominent arrays of parallel filaments containing filamentous actin. Surface membrane receptors such as integrins that mediate cell adhesion to extracellular matrix are known to have a central role in mechanotransduction and can generate mechanical signals that are known to propagate through the cytoplasm much more quickly than diffusion-based chemical signals (46).

Published reports suggest that adhesion receptors and their cytosolic partners can regulate trafficking of signaling proteins between the cytoplasm and nucleus, resulting in the control of transcription (47). Recently it has been shown that activation of MAP kinases can be controlled via integrins (48). Upon integrin-mediated adhesion to DPP, ERK translocates from the cytoplasm to the nucleus. Interestingly, this nuclear localization was abrogated in the presence of PD98059, an inhibitor specific for the phosphorylated form of ERK1/2. However, blocking with the RGD peptide also inhibited formation of the focal adhesion complex and the ERK1/2 signaling pathway. In control cells, ERK was localized in the cytoplasm. Published reports demonstrate that ERK accumulation in the nucleus occurs more efficiently in adherent cells, whereas nuclear accumulation of phosphorylated p38 and phosphorylated JNK are unaffected by changes in adhesion (49). In the nucleus, activated ERK efficiently phosphorylates ELK-1, and this is adhesion-dependent. Phosphorylated ELK-1 plays a pivotal role in immediate early gene induction by external stimuli (30). Our findings highlight the importance of cellular adhesion to DPP substrate activation of ERK, which translocates to the nucleus and transactivates the transcription factor ELK-1.

Cell anchorage to DPP substrate can have substantial effects on gene expression. Undifferentiated mesenchymal cells

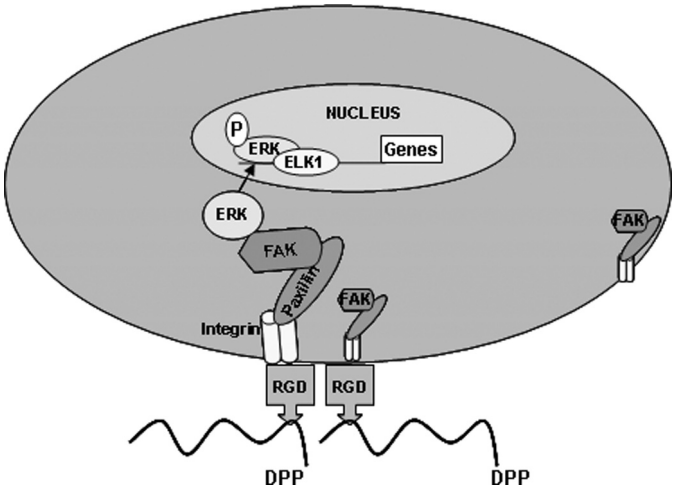

FIGURE 14. **Hypothetical model.** The hypothetical model depicts the RGD-mediated integrin anchorage of cells on DPP and the subsequent activation of focal adhesion complexes and downstream gene transcription.

anchored on DPP substrate had the ability to express transcription and growth factors like BMP4 and RUNX2 and odontogenic secretory stage-specific phenotypic markers like *DMP1* and *DSP*. The increase in the expression levels of these genes within 24 h suggests that cells attached to DPP matrix can activate transcriptional regulation and thereby aid in the differentiation process. Terminal differentiation of undifferentiated mesenchymal cells to functional odontoblast-like cells was confirmed by von Kossa and Alizarin Red staining of the extracellular matrix.

Taken together, these findings suggest that DPP plays a major role in anchorage-dependent signaling events. These events include physical coupling of integrins with extracellular DPP, which initiates a mechanical stimulus that results in the activation of FAK and paxillin and their interactions at the adhesion complex (Fig. 14). The ability of FAK to be present in focal adhesions as well as in the nucleus may be important for its role in regulating anchorage-dependent ERK activation. Once activated, the signals propagate through the cytoplasm, leading to accumulation of activated ERK in the nucleus where it phosphorylates transcription factors like ELK-1, leading to downstream odontogenic gene expression and differentiation of embryonic mesenchymal cells to odontoblast-like cells. The hallmark of terminal differentiation is the induction of mineralized matrix formation, which was confirmed by von Kossa and Alizarin Red staining in this study. Thus, extracellular DPP can provide a tight association between the structural and signaling elements in undifferentiated mesenchymal cells.

Acknowledgments—We are grateful to Drs. Sriram Ravindran, Tanvi Muni, and Qi Gao for providing assistance with the confocal imaging and cell culture.

REFERENCES

1. Feng, J. Q., Luan, X., Wallace, J., Jing, D., Ohshima, T., Kulkarni, A. B., D'Souza, R. N., Kozak, C. A., and MacDougall, M. (1998) Genomic organization, chromosomal mapping, and promoter analysis of the mouse dentin sialophosphoprotein (Dspp) gene, which codes for both dentin sialoprotein and dentin phosphoprotein. *J. Biol. Chem.* **273,** 9457–9464
2. Yamakoshi, Y., Lu, Y., Hu, J. C., Kim, J. W., Iwata, T., Kobayashi, K., Nagano, T., Yamakoshi, F., Hu, Y., Fukae, M., and Simmer, J. P. (2008) Porcine dentin sialophosphoprotein: length polymorphisms, glycosylation, phosphorylation, and stability. *J. Biol. Chem.* **283,** 14835–14844
3. George, A., Srinivasan, R., Thotakura, S. R., Liu, K., and Veis, A. (1999) Rat dentin matrix protein 3 is a compound protein of rat dentin sialoprotein and phosphophoryn. *Connect. Tissue Res.* **40,** 49–57
4. Yamakoshi, Y., Hu, J. C., Iwata, T., Kobayashi, K., Fukae, M., and Simmer, J. P. (2006) Dentin sialophosphoprotein is processed by MMP-2 and MMP-20 *in vitro* and *in vivo*. *J. Biol. Chem.* **281,** 38235–38243
5. Yamakoshi, Y., Hu, J. C., Fukae, M., Zhang, H., and Simmer, J. P. (2005) Dentin glycoprotein: the protein in the middle of the dentin sialophosphoprotein chimera. *J. Biol. Chem.* **280,** 17472–17479
6. Hart, P. S., and Hart, T. C. (2007) Disorders of human dentin. *Cells Tissues Organs* **186,** 70–77
7. MacDougall, M., Dong, J., and Acevedo, A. C. (2006) Molecular basis of human dentin diseases. *Am. J. Med. Genet.* **140,** 2536–2546
8. MacDougall, M., Simmons, D., Luan, X., Gu, T. T., and DuPont, B. R. (1997) Assignment of dentin sialophosphoprotein (DSPP) to the critical DGI2 locus on human chromosome 4 band q21.3 by *in situ* hybridization. *Cytogenet. Cell Genet.* **79,** 121–122
9. Thotakura, S. R., Mah, T., Srinivasan, R., Takagi, Y., Veis, A., and George, A. (2000) The non-collagenous dentin matrix proteins are involved in dentinogenesis imperfecta type II (DGI-II). *J. Dent. Res.* **79,** 835–839
10. Sreenath, T., Thyagarajan, T., Hall, B., Longenecker, G., D'Souza, R., Hong, S., Wright, J. T., MacDougall, M., Sauk, J., and Kulkarni, A. B. (2003) Dentin sialophosphoprotein knockout mouse teeth display widened predentin zone and develop defective dentin mineralization similar to human dentinogenesis imperfecta type III. *J. Biol. Chem.* **278,** 24874–24880
11. Suzuki, S., Sreenath, T., Haruyama, N., Honeycutt, C., Terse, A., Cho, A., Kohler, T., Müller, R., Goldberg, M., and Kulkarni, A. B. (2009) Dentin sialoprotein and dentin phosphoprotein have distinct roles in dentin mineralization. *Matrix Biol.* **28,** 221–229
12. D'Souza, R. N., Cavender, A., Sunavala, G., Alvarez, J., Ohshima, T., Kulkarni, A. B., and MacDougall, M. (1997) Gene expression patterns of murine dentin matrix protein 1 (Dmp1) and dentin sialophosphoprotein (DSPP) suggest distinct developmental functions *in vivo*. *J. Bone Miner. Res.* **12,** 2040–2049
13. Sabsay, B., Stetler-Stevenson, W. G., Lechner, J. H., and Veis, A. (1991) Domain structure and sequence distribution in dentin phosphophoryn. *Biochem. J.* **276,** 699–707
14. Linde, A., Bhown, M., and Butler, W. T. (1981) Non-collagenous proteins of rat dentin. Evidence that phosphoprotein is not covalently bound to collagen. *Biochim. Biophys. Acta* **667,** 341–350
15. Stetler-Stevenson, W. G., and Veis, A. (1983) Bovine dentin phosphophoryn: composition and molecular weight. *Biochemistry* **22,** 4326–4335
16. Veis, A. (1988) Phosphoproteins from teeth and bone. *Ciba Found. Symp.* **136,** 161–177
17. George, A., Bannon, L., Sabsay, B., Dillon, J. W., Malone, J., Veis, A., Jenkins, N. A., Gilbert, D. J., and Copeland, N. G. (1996) The carboxyl-terminal domain of phosphophoryn contains unique extended triplet amino acid repeat sequences forming ordered carboxyl-phosphate interaction ridges that may be essential in the biomineralization process. *J. Biol. Chem.* **271,** 32869–32873
18. Sfeir, C., and Veis, A. (1995) Casein kinase localization in the endoplasmic reticulum of the ROS 17/2.8 cell line. *J. Bone Miner. Res.* **10,** 607–615
19. Veis, A., Wei, K., Sfeir, C., George, A., and Malone, J. (1998) Properties of the $(DSS)_n$ triplet repeat domain of rat dentin phosphophoryn. *Eur. J. Oral Sci.* **106,** Suppl. 1, 234–238
20. Hao, J., Zou, B., Narayanan, K., and George, A. (2004) Differential expression patterns of the dentin matrix proteins during mineralized tissue formation. *Bone* **34,** 921–932
21. He, G., Ramachandran, A., Dahl, T., George, S., Schultz, D., Cookson, D., Veis, A., and George, A. (2005) Phosphorylation of phosphophoryn is crucial for its function as a mediator of biomineralization. *J. Biol. Chem.* **280,** 33109–33114
22. Alvares, K., Kanwar, Y. S., and Veis, A. (2006) Expression and potential role of dentin phosphophoryn (DPP) in mouse embryonic tissues involved

in epithelial-mesenchymal interactions and branching morphogenesis. *Dev. Dyn.* **235,** 2980–2990
23. Jadlowiec, J., Koch, H., Zhang, X., Campbell, P. G., Seyedain, M., and Sfeir, C. (2004) Phosphophoryn regulates the gene expression and differentiation of NIH3T3, MC3T3-E1, and human mesenchymal stem cells via the integrin/MAPK signaling pathway. *J. Biol. Chem.* **279,** 53323–53330
24. Malik, R. K., and Parsons, J. T. (1996) Integrin-dependent activation of the p70 ribosomal S6 kinase signaling pathway. *J. Biol. Chem.* **271,** 29785–29791
25. Tilghman, R. W., Slack-Davis, J. K., Sergina, N., Martin, K. H., Iwanicki, M., Hershey, E. D., Beggs, H. E., Reichardt, L. F., and Parsons, J. T. (2005) Focal adhesion kinase is required for the spatial organization of the leading edge in migrating cells. *J. Cell Sci.* **118,** 2613–2623
26. Golubovskaya, V., Kaur, A., and Cance, W. (2004) Cloning and characterization of the promoter region of human focal adhesion kinase gene: nuclear factor κB and p53 binding sites. *Biochim. Biophys. Acta* **1678,** 111–125
27. Cance, W. G., and Golubovskaya, V. M. (2008) Focal adhesion kinase versus p53: apoptosis or survival? *Sci. Signal.* **1,** pe22
28. Mamali, I., Kotsantis, P., Lampropoulou, M., and Marmaras, V. J. (2008) Elk-1 associates with FAK, regulates the expression of FAK and MAP kinases as well as apoptosis in HK-2 cells. *J. Cell. Physiol.* **216,** 198–206
29. Howe, A. K., Aplin, A. E., and Juliano, R. L. (2002) Anchorage-dependent ERK signaling—mechanisms and consequences. *Curr. Opin. Genet. Dev.* **12,** 30–35
30. Aplin, A. E., Stewart, S. A., Assoian, R. K., and Juliano, R. L. (2001) Integrin-mediated adhesion regulates ERK nuclear translocation and phosphorylation of Elk-1. *J. Cell Biol.* **153,** 273–282
31. Geiger, B., Spatz, J. P., and Bershadsky, A. D. (2009) Environmental sensing through focal adhesions. *Nat. Rev. Mol. Cell Biol.* **10,** 21–33
32. Engler, A. J., Sen, S., Sweeney, H. L., and Discher, D. E. (2006) Matrix elasticity directs stem cell lineage specification. *Cell* **126,** 677–689
33. Gilbert, P. M., Havenstrite, K. L., Magnusson, K. E., Sacco, A., Leonardi, N. A., Kraft, P., Nguyen, N. K., Thrun, S., Lutolf, M. P., and Blau, H. M. (2010) Substrate elasticity regulates skeletal muscle stem cell self-renewal in culture. *Science* **329,** 1078–1081
34. Hynes, R. O. (2004) The emergence of integrins: a personal and historical perspective. *Matrix Biol.* **23,** 333–340
35. Giancotti, F. G., and Ruoslahti, E. (1999) Integrin signaling. *Science* **285,** 1028–1032
36. Ruoslahti, E. (1988) Fibronectin and its receptors. *Annu. Rev. Biochem.* **57,** 375–413
37. Ruoslahti, E. (1996) Integrin signaling and matrix assembly. *Tumour Biol.* **17,** 117–124
38. Staquet, M. J., Couble, M. L., Roméas, A., Connolly, M., Magloire, H., Hynes, R. O., Clezardin, P., Bleicher, F., and Farges, J. C. (2006) Expression and localisation of αv integrins in human odontoblasts. *Cell Tissue Res.* **323,** 457–463
39. Mamali, I., Kapodistria, K., Lampropoulou, M., and Marmaras, V. J. (2008) Elk-1 is a novel protein-binding partner for FAK, regulating phagocytosis in medfly hemocytes. *J. Cell. Biochem.* **103,** 1895–1911
40. Kornberg, L., Earp, H. S., Parsons, J. T., Schaller, M., and Juliano, R. L. (1992) Cell adhesion or integrin clustering increases phosphorylation of a focal adhesion-associated tyrosine kinase. *J. Biol. Chem.* **267,** 23439–23442
41. Lim, S. T., Chen, X. L., Lim, Y., Hanson, D. A., Vo, T. T., Howerton, K., Larocque, N., Fisher, S. J., Schlaepfer, D. D., and Ilic, D. (2008) Nuclear FAK promotes cell proliferation and survival through FERM-enhanced p53 degradation. *Mol. Cell* **29,** 9–22
42. Turner, C. E. (1991) Paxillin is a major phosphotyrosine-containing protein during embryonic development. *J. Cell Biol.* **115,** 201–207
43. Brown, M. C., West, K. A., and Turner, C. E. (2002) Paxillin-dependent paxillin kinase linker and p21-activated kinase localization to focal adhesions involves a multistep activation pathway. *Mol. Biol. Cell* **13,** 1550–1565
44. Turner, C. E. (2000) Paxillin and focal adhesion signalling. *Nat. Cell Biol.* **2,** E231–E236
45. Shemesh, T., Bershadsky, A. D., and Kozlov, M. M. (2005) Force-driven polymerization in cells: actin filaments and focal adhesions. *J. Phys. Condens. Matter* **17,** S3913–S3928
46. Jaalouk, D. E., and Lammerding, J. (2009) Mechanotransduction gone awry. *Nat. Rev. Mol. Cell Biol.* **10,** 63–73
47. Juliano, R. L., Aplin, A. E., Howe, A. K., Short, S., Lee, J. W., and Alahari, S. (2001) Integrin regulation of receptor tyrosine kinase and G protein-coupled receptor signaling to mitogen-activated protein kinases. *Methods Enzymol.* **333,** 151–163
48. Aplin, A. E., Hogan, B. P., Tomeu, J., and Juliano, R. L. (2002) Cell adhesion differentially regulates the nucleocytoplasmic distribution of active MAP kinases. *J. Cell Sci.* **115,** 2781–2790
49. Aplin, A. E. (2003) Cell adhesion molecule regulation of nucleocytoplasmic trafficking. *FEBS Lett.* **534,** 11–14